REPORT DOCUMENTATION PAGE

Form Approved
OMB NO. 0704-0188

1. AGENCY USE ONLY (Leave Blank)	2. REPORT DATE 04/04/2005	3. REPORT TYPE AND DATES COVERED Final Report 07/01/2004-03/31/2005

4. TITLE AND SUBTITLE
Energy Absorption Behaviors of Nanoporous Systems

5. FUNDING NUMBERS
W911NF-04-1-0244

6. AUTHOR(S)
Yu Qiao

7. PERFORMING ORGANIZATION NAME(S) AND ADDRESS(ES)
The University of Akron
Polsky Bldg., Rm 284, Akron, OH 44325-2102

8. PERFORMING ORGANIZATION REPORT NUMBER
The University of Akron

9. SPONSORING / MONITORING AGENCY NAME(S) AND ADDRESS(ES)

U. S. Army Research Office
P.O. Box 12211
Research Triangle Park, NC 27709-2211

10. SPONSORING / MONITORING AGENCY REPORT NUMBER

46476.1-MS

11. SUPPLEMENTARY NOTES
The views, opinions and/or findings contained in this report are those of the author(s) and should not be construed as an official Department of the Army position, policy or decision, unless so designated by other documentation.

12 a. DISTRIBUTION / AVAILABILITY STATEMENT

Approved for public release; distribution unlimited.

12 b. DISTRIBUTION CODE

13. ABSTRACT (Maximum 200 words)

In this exploratory research program we investigated the energy absorption behaviors of systems consisting of hydrophobic nanoporous silica particles immersed in liquids. The two principal goals are (1) validating the concept of the use of nanoporous materials in energy absorption systems; and (2) identifying the optimum surface species. During the 9 month of ARO support much progress has been made on both of the goals. In the following, we describe the achievements. The future directions are also discussed.

14. SUBJECT TERMS	15. NUMBER OF PAGES 16
	16. PRICE CODE

17. SECURITY CLASSIFICATION OR REPORT	18. SECURITY CLASSIFICATION ON THIS PAGE	19. SECURITY CLASSIFICATION OF ABSTRACT	20. LIMITATION OF ABSTRACT
UNCLASSIFIED	UNCLASSIFIED	UNCLASSIFIED	UL

REPORT DOCUMENTATION PAGE (SF298)
(Continuation Sheet)

I. Publications Supported by The Army Research Office

(a) Papaers published in or accepted by peer-reviewed journals:

1. Kong X, Qiao Y. Performance of a nanoporous energy absorption system under cyclic loading. *Appl. Phys. Lett.*, in the press.
2. Kong X, Surani FB, Qiao Y. Effects of addition of ethanol on the infiltration pressure of a mesoporous silica. *J. Mater. Res.*, in the press.
3. Kong X, Qiao Y. Thermal effect on pressure induced infiltration of a nanoporous system. *Phil. Mag. Lett.*, in the press.
4. Qiao Y, Kong X (2005). Modeling of the kinetics of confined nonwetting flow in a mesoporous particle. *Phys. Scripta*, **71**, 27-30.

(b) Papers submitted

5. Kong X, Qiao Y. Pressure induced infiltration in nanopores. *Appl. Phys.*, to be published.
6. Kong X, Surani FB, Qiao Y. Energy absorption of nanoporous silica particles in aqueous solutions of sodium chloride. *Phys. Scripta*, to be published.
7. Qiao Y, Kong X. Effective dewetting in a microporous particle. *J. Fluid Eng.*, to be published.

II. Demographic Data for this Reporting Period:

(a) Number of Manuscripts submitted during this reporting period: 0
(b) Number of Peer Reviewed Papers submitted during this reporting period: 7
(c) Number of Non-Peer Reviewed Papers submitted during this reporting period: 0
(d) Number of Presented but not Published Papers submitted during this reporting period: 0

III. Scientific Progress and Acomplishments

A. Introduction

The advanced energy absorption systems (EAS) have immense importance to a variety of protection applications for soldiers and critical parts subjected to dynamic loadings. Many of them are based on "soft" materials that can sustain multiple-site and widespread damages or phase transformations, through which the energy can be dissipated and thus extensive damages in the structures to be protected are avoided. However, currently, the capacity of energy absorption of EAS, although already close to its limit, is still far from satisfactory. To produce EAS of superior energy absorption efficiency, new mechanisms must be discovered.

When a nonwetting liquid is forced to "flow" into a nanoporous material under an external pressure, due to the ultrahigh specific surface area, a large amount of energy can be transformed into the solid-liquid

interfacial tension. Although this has been well appreciated in the chemical, environmental, and bioscience fields for the catalysis and selective absorption applications, there are few attempts to apply it in mechanical protection systems. In view of these considerations, we carried out an exploratory research on the development of nanoporous energy absorption systems (NEAS) consisting of nanoporous particles immersed in non-wetting liquids.

Nanoporous materials can be considered as nanovoid-surrounding networks usually covalently crosslinked together, with the gas-solid interfaces as the most dominant characteristic [1]. There are a variety of nanoporous organic-inorganic hybrids in nature, e.g. diatoms, radiolarii, and abalone shell, exhibiting synergistic properties. Other examples include the nanoporous foams in lungs permitting the exchange of oxygen between the air and the blood, and various photonic materials such as butterfly wings. Since the last century a number of synthetic nanoporous materials have been developed, especially in the past two decades. The small pore size and the large pore volume fraction in the nanoporous materials lead to the very high area/mass ratio in the range of 100-2000 m^2/g, which, together with the excellent cost-performance balance, makes them attractive for the sorption and catalysis applications. The most commonly used synthesis method is the templating technique, in which the network surrounding the template is produced first through phase separation or nanocasting, and then the template is removed by etching or heating, as depicted in Fig.1.

The nanoporous materials can be classified into (1) microporous materials with the pore size below 2 nm, (2) mesoporous materials with the pore size in the range of 2-50 nm, and (3) macroporous materials with the pores larger than 50 nm but smaller than 1000 nm [2]. The synthetic nanoporous materials are often of the ordered microstructure with the nearly uniform pore size and pore shape distribution, resulting in the somewhat homogeneous properties. However, due to the grain packing and additional microporosity, the porosity can vary in a broad range. Most of these materials are inorganic, including oxide-type materials such as silica and titania, carbon materials, binary compounds such as sulfides and nitrides, and porous metals. The organic nanoporous materials include polyurethane and polypyrrole.

B. Basic Consideration of Mechanisms

When nanoporous particles are immersed in a non-wetting liquid, the liquid cannot enter the nanopores spontaneously. With the increase in external pressure, however, as the capillary effect is overcome, the liquid can be forced to infiltrate into the nanoporous material, as depicted in Fig.2. Because of the factors that are still under investigation, as the pressure is reduced, in a certain types of nanoporous materials the confined liquid would remain in the nominally energetically unfavorable nanopores, and thus the excess solid-liquid interfacial energy can be considered as being "absorbed". Due to the large specific surface area, the energy absorption effectiveness of this system can be higher than 10 J/g. Furthermore, since the sizes of the nanoporous particles are usually at the μm or sub-μm level, the characteristic time of the infiltration process is around 10^{-9}-10^{-7} sec., making this technique attractive for high-strain-rate applications.

All the previous studies in this area are merely proof-of-concept quasi-static experiments [3,4]. The effects of important factors, such as strain rate, pore size distribution, surface structures, pore volume fraction, particle size, and admixtures, are still inadequately understood. The conventional interface theories and microfluid mechanics have failed to explain the experimental results. The predictions of infiltration pressure of the classic capillary theory could be several times lower than the measured data. More importantly, there is still no satisfactory model that can capture the phenomenon of "nonoutflow".

To understand the sorption properties of nanoporous materials, a number of researches have been performed on the molecular behaviors in nanopores. Through the nuclear magnetic resonance (NMR) experiments, it was confirmed that, in a mesopore, there is an interface layer with the thickness of 0.5-5 nm near the solid-liquid interface, as depicted in Fig.3 [5]. In the interface layer surface diffusion is dominant, while in the interior the single-file diffusion model can describe the molecular behavior quite well. The average diffusion distance of the liquid molecules can be stated as $\langle x^2 \rangle = \tilde{\alpha} t + \tilde{\beta} t^k$, with t being time and $\tilde{\alpha}$, $\tilde{\beta}$, and k being material constants. The time scale within which the difference between the two types of diffusion is significant can be measured by the retention time, t_r, the required time that it takes for the interface layer to be replaced by the molecules from the interior.

When the liquid enters a nanoporous particle, in addition to the change in interfacial energy, a certain amount of energy will be dissipated due to the internal friction. For instance, Li [6] noticed that the energy dissipation was quite significant when water "flew" from the compressed region to the tensile region in a saturated hydrophilic nanoporous silica plate.

C. Energy absorption behaviors of a mesoporous silica under cyclic loadings

For the direct observation of infiltration behaviors of nanoporous materials, we designed a simple transparent poly(methyl methacrylate) (PMMA) system (see Fig.2). The material under investigation was an end-capped Fluka 100 C_8 reversed phase mesoporous silica with the average pore size $\bar{r} = 7.8$ nm and the standard deviation $\delta r = 2.4$ nm. The specific pore volume was 560 mm^3/g, and the specific area was 287 m^2/g. The Barrett-Joyner-Halenda (BJH) adsorption characterization measurement was performed at the Quantachrome Instruments. The surface coverage was 10-12% ($\pm$ 4 $\mu mol/m^2$), which led to a high degree of hydrophobicity. The particle size was in the range of 15-35 μm. Prior to the infiltration tests, the silica particles had been calcinated in air at 150°C for 12 hours.

The aqueous suspension of 0.5 g of the mesoporous silica particles was sealed in a PMMA cylinder by a stainless steel piston with reinforced gaskets. Initially, no air bubble could be observed. The infiltration experiment was performed using an Instron 5569 machine. The piston was first compressed into the container at a constant rate of 1.0 mm/min. Once the pressure exceeded about 50 MPa, the crosshead was moved back at the same speed. The loading-unloading cycle was repeated until the absorption isotherm curves converged to the steady-state, as shown by curves (a, b) in Fig.3, where the specific volume variation is defined as $\Delta V_0/W$, with ΔV_0 being the volume change of the system and W the weight of the silica particles. The system was then thermally treated in a temperature bath in the range of 30-80°C for 0.5 hour either (1) immediately or (2) after resting at room temperature for 6-24 hours, followed by another loading-unloading test. The testing results are shown by curves (c, d) in Fig.3, respectively. Altogether four samples were tested.

Curve (a) in Fig.3 shows that, following the initial linear stage, as the pressure reached the infiltration pressure, $p_{in} \approx 17$ MPa, the water was forced into the nanopores, causing the large increase in system compressibility. If the pore size were perfectly uniform, the plateau should be flat. In the current system, due to the pore size distribution, the slope of the absorption isotherm was finite. Eventually, at about 30 MPa, most of the pores were filled and the system compressibility decreased rapidly. The volume variation associated with the plateau region was about 0.55 cm^3/g, close to the BJH result of the specific pore volume. As the pressure was reduced, the confined water remained in the nanopores, and thus the

unloading curves were quite linear. During the loading-unloading process, there was no significant change in system appearance, except for the variation in volume, indicating that the gas entrapped in the nanopores dissolved in the liquid phase. Since no air bubble could be observed even when the pressure was reduced back to the atmosphere pressure, the gas content in the liquid phase outside the nanoporous particles must be quite constant, that is, the dissolved gas molecules remained in the nanopores. Because of the "nonoutflow", the extent of infiltration was considerably lowered in the following loading-unloading cycles (see curve b in Fig.3).

When, immediately after the first loading-unloading cycle, the system was thermally treated, the liquid phase was still clear and little air bubbles were formed. However, the energy absorption capacity of the system was recovered significantly (see curve c in Fig.3 and Table 1), indicating clearly that after the thermal treatment a certain portion of the porous space was occupied by the gas phase. When the temperature exceeded 50°C, the system could be almost fully recovered.

If, on the other hand, after the first infiltration cycle, the specimen was rested at room temperature under p_{at}, the system appearance would change gradually. After 6 hours, a large number of air bubbles with the sizes in the range of 0.05 mm to 0.5 mm were formed and therefore the sample was no longer transparent. After 24 hours, the total volume of the air bubbles was estimated as 0.25 cm^3/g, while the energy absorption capacity was still close to zero, suggesting that the nanopores were still filled by liquid. Thermally treating this system would cause a partial recovery, as shown by curve (d) in Fig.3, where the system recoverability, R_p, is defined as E^*_t/E^*_1, with E^*_t being the absorbed energy in the loading-unloading cycle subsequent to the postponed thermal treatment; the treatment temperature was set to 70°C; and t_r is the room-temperature resting time. Clearly, during the resting period, a certain amount of gas molecules diffused out of the nanopores, and the decrease in system recoverability should be attributed to the reduction of the excess gas content in the nanoenvironment.

D. Effects of addition of promoters

One of the vital factors dominating the system performance is the infiltration pressure, p_{in}. In an impact test, only the energy carried by the portion of incident pulse with the pressure higher than p_{in} can be dissipated by the nanoporous system, that is, the energy absorption is selective. This characteristic is beneficial to minimizing the weights and sizes of protection systems that can filter out the "peaks" of stress waves and let the harmless low-stress portions bypass. However, currently, the researches in this area are limited to systems based on pure water, in which p_{in} is primarily determined by the surface treatment techniques and the pore sizes. One promising method to adjust p_{in} is to use chemical admixtures as promoters.

The admixture should be of the following characteristics: (1) the molecules are much smaller than the pore size such that the "repelling" effect is negligible; (2) the molecules are capable to form strong bonds with water; and (3) it is energetically favorable for the admixture molecules to enter the nanopores. Based on these criteria, ethanol is an attractive candidate. Ethanol is a material commonly used in industry. The chemical formula is C_2H_5OH, with the atomic weight of 46.07 amu. At p_{at}, it is in liquid form in the temperature range of -114.3°C to 78.4°C, and at room temperature the weight density is 789 kg/m^3. The molecular size of ethanol is comparable with that of water. It is easily soluble in water; and it is wetting to silica even after surface treatments.

There are two possible results when the mesoporous particles are immersed in an aqueous solution of ethanol. The first is selective absorption, that is, only ethanol molecules can enter the nanopores. Under

this condition, ethanol would fail to promote the water infiltration. The second possibility is the desired mixed infiltration, i.e. the ethonal and water molecules enter the nanopores simultaneously. Due to the confinement effect of pore walls, it is not clear whether the composition of the confined liquid inside the nanopores is the same as outside.

The mesoporous silica particles were immersed in a mixture of Pharmco 95% ethanol and distilled water, and sealed in a 304 stainless steel container. The volume fraction of ethanol in the liquid phase, c, was in the range of 0 to about 50%. Similar with the behavior of the pure water based system, as the load, P, increased, the piston was pressed into the container and at the critical pressure, p_{in}, the pressure induced infiltration occurred. As the load was reduced back to zero, the "nonoutflow" of the confined liquid caused a pronounced hysteresis of the absorption isotherm, as shown in Fig.4.

It was found that when c was higher than about 50%, infiltration could occur spontaneously at atmosphere pressure. When c was relatively low, the infiltration pressure was positive. The results of p_{in} are shown in Fig.5 as a function of c. After the loading-unloading infiltration test, the liquid was filtered by an AMTS 40-60 filter so as to remove the silica particles. Then, its composition was analyzed by a Shimadzu GC-17A gas chromatography analyzer equipped by an Rtx-5 flame ionization detector, and the results are given in Fig.5. The injection volume was 0.1 μl; the temperatures of the column, the injection part, and the detector were 110°C, 220°C, and 300°C, respectively. The carrier gas was nitrogen and the flow rate was 1.4 ml/min.

As the ethanol content increases, it can be seen that there is a consistent decrease in infiltration pressure. The width of the plateau region, however, is quite insensitive to the variation in c, indicating that the addition of ethanol does not affect the accessibility of pore surfaces. According to Fig.5, the relationship between the infiltration pressure and the ethanol content is quite nonlinear, which is different from the results of conventional interface theories. Since ethanol molecules are neutral, at an infinity large interface, the acid and base components of the Lewis acid-base interaction are nearly constant, and therefore the degree of nonlinearity of concentration dependence of interface energy is low. The nonlinear phenomenon observed in the nanoporous system demonstrates that the heterogeneous structure of the confined liquid in nanopores must be taken into consideration.

Figure 6 shows that, after the infiltration test, the ethanol content outside the nanoporous particles is decreased. Thus, the ethanol concentration of the confined liquid must be higher, that is, the infiltration of the aqueous solution of ethanol can be considered as a combination of selective absorption and mixed absorption. The difference between the ethanol contents before and after the infiltration tests, c and c^*, is around 4.3%. This value is quite insensitive to c. The systems tested in the current study consisted of 0.5 g of nanoporous silica particles, and the total pore volume $V_p = 0.27$ cm^3. The liquid volume $V_l = 2.90$ cm^3. Hence, according to mass conservation, the 4.3% difference between c and c^* should be balanced by the increase in ethanol concentration of confined liquid by 42%, which must be related to the heterogeneous interface layer structure.

Assume that the liquid composition in the interior of a nanopore is the same as c^*, the ethanol concentration in the interface layer, c_i, can be assessed as $[1+8.8r^2/(2rd-d^2)]\cdot x$, where $x = 4.3\%$ is the difference between c and c^*. If r is taken as 7.8 nm, when $d \approx 1.5$ nm, c_i tends to 100%. Under this condition, the confined liquid consists of a saturated ethanol layer at the solid-liquid interface and a bulk phase in the interior. Note that the actual structure is likely in between the fully heterogeneous case and the fully homogeneous case.

E. Effects of addition of recovery agents

In the systems discussed above, once the liquid enters the nanopores, it cannot come out even when the pressure is reduced to 0, and thus the system can be used only once. In order to develop reusable protection devices, we investigated the effects of addition of recovery agents. As will be analyzed in Section V, a recovery agent can be a chemical that lowers the gas solubility, for which sodium chloride (NaCl) is a promising candidate.

The mesoporous silica particles were dispersed in an aqueous solution of NaCl. By measuring the piston displacement, the volume variation of the energy absorption system was obtained as a function of the pressure. A number of energy absorption systems with the NaCl concentrations, c, in the range of 0-25.9wt.% were studied. At each NaCl concentration, 3-4 samples were tested.

The first loading-unloading cycle of NaCl modified system was quite similar with that of pure water based systems. In the second cycle, however, the specific absorbed energy was largely increased, as shown in Fig.7. It is clear that the confined liquid consists of two parts: reversible part and irreversible part. The reversible part is probably related to the liquid in larger pores that can come out once the applied pressure is removed, and the associated porous space can be refilled. The irreversible part, on the other hand, remains in the nanopores even when the pressure is reduced to 0. This phenomenon leads to an 80% decrease in energy absorption efficiency in the pure water based system (see Fig.3b). As the NaCl concentration becomes higher, through Figs.7 and 8, it can be seen that the fraction of the reversible part increases, that is, the recoverability of the system is improved. The recoverability, E_i/E_1, where E_i is the specific absorbed energy in the i^{th} loop ($i = 2, 3, 4\ldots$), is sensitive to the NaCl concentration when c is in the range of 5-17wt.%. When the NaCl concentration is higher than 17wt%, the recoverability remains around 75%, and the influence of further increase in c is negligible. Under this condition, the loss of the specific absorbed energy is only about 25%, 3 times lower than that in a pure water based system.

At the macroscopic scale, since the NaCl solution is neutral and the acid and base terms are quite constant, the interfacial energy is nearly linear to the NaCl concentration.[13,14] According to the experimental data obtained in the current study, however, similar with the behaviors of the ethanol modified system, the NaCl concentration dependences of P_{out}, E_i, and E_i/E_1 are all highly nonlinear, indicating that the conventional interface theories cannot be applied for the nanoenvironment. This phenomenon should be related to the confinement effect of the pore walls.

F. Dynamic testing

In order to understand the NEAS performance at high strain rates, a dynamics experiment was performed using a Hopkinson bar. The speed of the striker was 6 m/s. The reference curve was obtained by measuring the output pulse of a system similar to that depicted in Fig.2(a) but containing only pure water. The dissipated energy of such a system was negligible, as it should. Then, by adding 0.7 g of nanoporous silica particles, the dynamic energy absorption associated with the pressure induced water infiltration was measured. Immediately after the first impact experiment of the NEAS, the same system was tested again so as to evaluate the recoverability. The experimental results of the output pulses are shown in Fig.9.

The peak stress of the output pulse of water was about 100 MPa, and that of the NEAS was only around 35 MPa, indicating that most of the energy carried by the compressive pulse was dissipated. This can be attributed to that, since the particle size is 15-35 μm, the characteristic infiltration time is at the sub-μs

level, and thus the energy absorption effectiveness remains large at a high strain rate. Actually, compared with the quasi-static case, the energy absorption effectiveness increases slightly as the strain rate rises, probably due to the increase in internal friction.

An interesting phenomenon is that, in the dynamic test, even without using any chemical admixtures, the system recoverability is nearly 100%, that is, after the first impact test, the energy absorption effectiveness of the NEAS is almost unchanged. This is very different from the result of the quasi-static experiment, the reason for which is still unclear.

G. A Thermodynamics Analysis of Defiltration Process

The motion of the gas-liquid contact line in a nanopore can be considered as the result of expansion or shrinkage of the gas phase. Note that at the nm level, sharp liquid-gas interfaces may not exist. Nevertheless, effective boundaries can be defined, e.g. in the context of Gibbs dividing surfaces, as shown in Fig.10. In an initially filled nanopore, the formation of a gas phase nucleus increases the free energy of system by (a) $\Delta\mu \cdot V_G$, where $\Delta\mu$ is the specific nucleation energy and $V_G = \pi r^2 h$ is the volume of the gas phase, with h being the nucleus length; (b) $\gamma_{GL} \cdot A_{GL}$, where γ_{GL} is the surface tension of the liquid and $A_{GL} = 2\pi r^2$ is the gas-liquid interface area; and (c) the external work $p \cdot \Delta V$, where p is the applied pressure and $\Delta V = V_G$ is the system volume change. On the other hand, with the nucleation of the gas phase, since the liquid is nonwetting, the liquid-solid interfacial energy is reduced by $\Delta\gamma A_{GS}$, where $\Delta\gamma$ is the difference between the gas-solid and liquid-solid interfacial energy, and $A_{GS} = 2\pi rh$ is the gas-solid interface area. Note that, if the effective gas-liquid interfaces are irregular, geometry factors should be used in the calculations of A_{GL} and V_G, which are ignored in the following discussion for the sake of simplicity.

The thermodynamics equilibrium condition can then be stated as

$$\Delta\mu \cdot V_G + \gamma_{GL} \cdot A_{GL} + p \cdot \Delta V = \Delta\gamma A_{GS}, \tag{1}$$

which can be rewritten as

$$r = r_{cr} \text{ or } h = h_{cr} \tag{2}$$

where $r_{cr} = \dfrac{2\Delta\gamma}{(p + \Delta\mu) + 2\gamma_{GL}/h}$ is the critical pore radius and $h_{cr} = \dfrac{2\gamma_{GL}}{2\Delta\gamma/r - (p + \Delta\mu)}$ is the critical nucleus size of gas phase. According to Eq.(2), when $r < r_{cr}$, the gas phase is stable and can expand spontaneously, which eventually leads to the "outflow"; when $r > r_{cr}$, the liquid-to-gas phase transformation is energetically unfavorable and therefore the gas phase nucleus will vanish, resulting in the "nonoutflow".

The value of $\Delta\gamma$ is estimated as $p_{in}\bar{r}/2$, and $\Delta\mu$ is taken as $\mu_0 \cdot \rho_G$, where $\mu_0 = 2257.1$ J/kg is the specific energy of evaporation of water and ρ_G is the density of gas phase, which, if we assume that the gas phase follows the law of ideal gas, can be assessed as $\rho_G = \rho_0/(1+p/p_{at})$, with $\rho_0 = 1.21$ kg/m^3 being the air density at p_{at}. For the first-order approximation, the macroscopic value of γ_{GL}, 72 mJ/m^2, is used. The results are shown in Fig.11. According to Eq.(2), there exists an ultimate pore size $r_{ul} = \dfrac{2\Delta\gamma}{p + \Delta\mu}$, at which $h_{cr} \to \infty$. If $r > r_{ul}$, the "outflow" is impossible for any $\{\Delta\gamma, \Delta\mu, \gamma_{GL}, p\}$.

Based on a Fourier Transform Infrared Spectroscopy (FTIR) analysis, it was confirmed that, at liquid-solid interfaces, there exist a large number of nm-scale gas phase nuclei [7]. As temperature rises, the fraction of bigger nuclei increases, i.e. the average h is larger, which explains that, under p_{at}, while at room

temperature the "outflow" was negligible, when $T > 50^{\circ}C$ the gas phase nucleation and growth could occur. After the room-temperature resting, however, due to the significant decrease in gas content in the nanopores, the average size of gas phase nuclei is smaller, and therefore the same thermal treatment can cause only a reduced system recovery.

It is clear that the above analysis, which is in context of mean-field theory, does not constitute a fully developed model. A number of details such as the kinetics of gas phase nucleation and growth, the possible fragment of gas/liquid phases, and the gas density dependence of $\{\Delta\gamma, \Delta\mu, \gamma_{GL}\}$, are not taken into account. Furthermore, this model can be used only for the "outflow" process, since the "inflow" is dominated by the kinetics of gas-liquid phase transformation. Nevertheless, this model captures the pore size effect on the "nonoutflow" quite successfully, which provides a scientific basis for further discussion.

IV. Conclusions

Through the 9-month research supported by The Army Research Office, the fundamental issues of the pressure induced infiltration of nanoporous materials are much better understood. It has been demonstrated experimentally that the use of nanoporous materials in energy aborption systems is a promising technique. The following conclusions are drawn:

(1) The efficiency of energy absorption of a nanoporous system can be higher than that of conventional protection materials by orders of magnitude.
(2) Chemical admixtures that can form strong bondings with both water molecules and pore walls can be used as promoters to adjust infiltration pressures, based on which selective protection systems can be designed.
(3) Chemical admixtures that can lower gas solubility can be used as recovery agents such that the nanoporous energy absorption system can be used repeatedly.
(4) Under a high strain rate, the efficiency of energy absorption of the nanoporous system increases.
(5) The infiltration and defiltration of nanoporous materials cannot be analyzed in context of conventional interface theory and microfluid mechanics. The confinement effect of pore walls and the mass/energy exchanges between gas and liquid phases must be taken into consideration.

V. Future Directions of Research

While excitng results have been achieved in the exploratory research, the study on nanoporous energy absorption systems is still far from being complete. Since the surface area of the mesoporous silica is relatively low and the porous structure is poorly designed, the experiments discussed above do not represent fully developed systems. The effectiveness of a number of important factors, such as the surface groups, the pore size distribution, the particle size distribution, the pore volume fraction, the admixtures, are still inadequately understood, imposing tremendous difficulties in system optimization. More importantly, for the behaviors of nanoporous systems subjected to high strain rates, not only the theoretical analyses but also the experimental data are scarce. In order to develop the high-performance protection systems, systematic investigations on these variables must be performed.

In additon to the hydrophobic silica discussed above, similar energy absorption results have also been obsered in experiments of various silicalites and nanoporous carbons. The liquid phase can be either water based or liquid metal based. We propose to carry out a comprehensive study on the promising materials so as to provide a scientific basis for materials selection.

References

[1] Polarz S, Smarsly B. *J Nanosci Nanotech* **2**: 581 (2002).
[2] Rouquerol J et al. *Pure Appl Chem* **66**: 1739 (1994).
[3] Eroshenko V, Regis RC, Soulard M, Patarin J. *J Am Chem Soc* **123**: 8129 (2001).
[4] Martin T et al. *Chem Commun*: 24 (2002).
[5] Kimmich R. *Chem Phys* **284**: 253 (2002).
[6] Li JCM. *J Alloys Comp* **310**: 24 (2001).
[7] Miller JD, Hu YH, Veeramasuneni S, Lu Y. *Colloid Surface* **A154**: 137 (1999).

Table 1 The system recoverability, $R_s = E^*_2/E^*_1$, as a function of the thermal treatment temperature, T, where E^*_i is the absorbed energy in the i-th loading-unloading cycle (i = 1,2).

T (°C)	21	30	40	50	70	80
R_s (%)	11.3	24.4	45.0	94.3	97.4	97.0

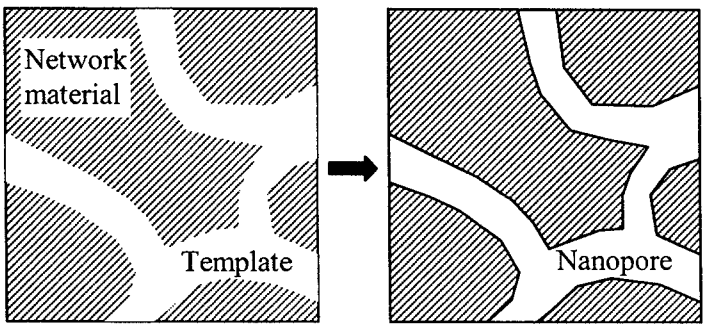

Fig.1 A schematic representation of the synthesis of a nanoporous material by removing the template.

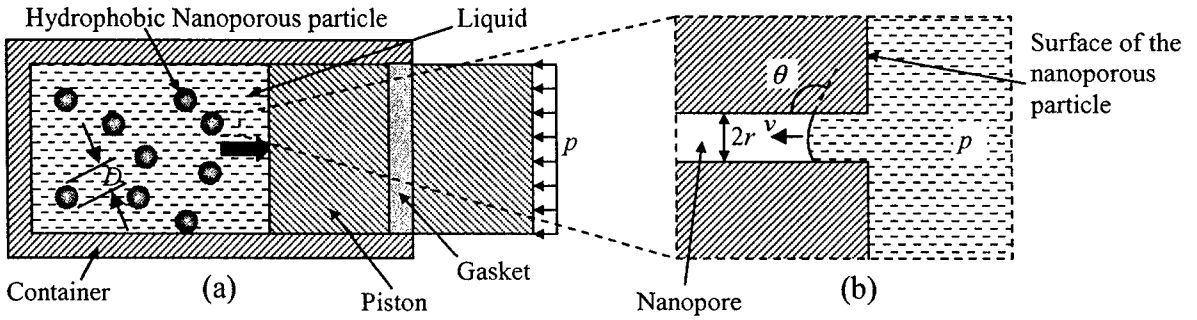

Fig.2 Schematic diagrams of (a) the system consisting of hydrophobic nanoporous particles immersed in a liquid; and (b) the forced "flow" in a nanopore.

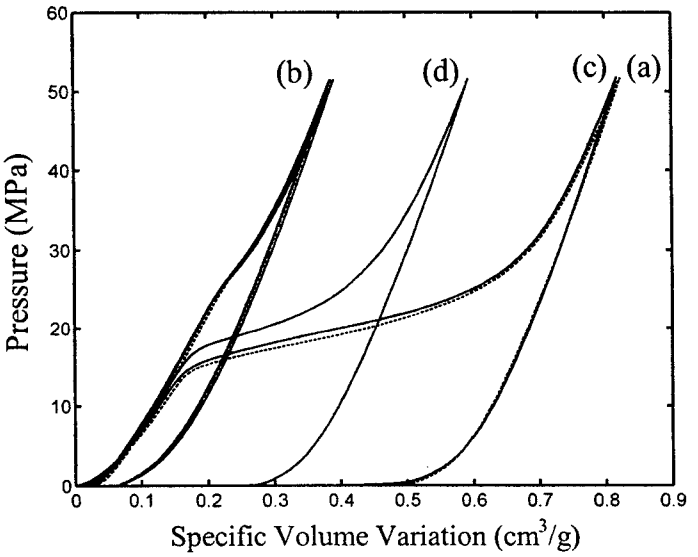

Fig.3 The energy absorption isotherms: (a) the first loading-unloading cycle; (b) the second, the third, and the fourth loading-unloading cycles without thermal treatment; (c) after the immediate thermal treatment; and (d) after the postponed thermal treatment.

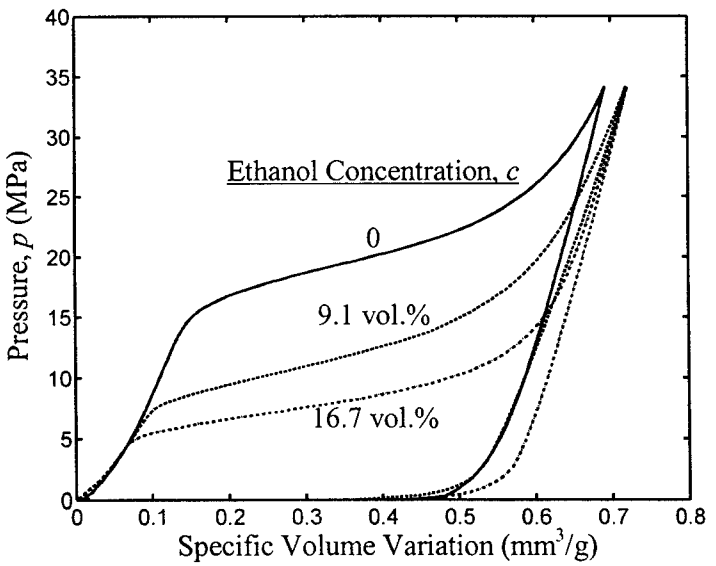

Fig.4 The sorption isotherm curves at various ethanol concentrations.

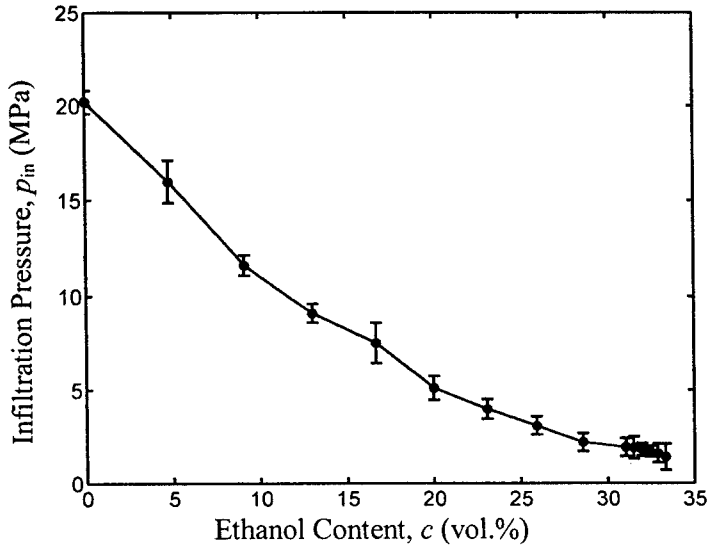

Fig.5 The infiltration pressure as a function of the ethanol concentration.

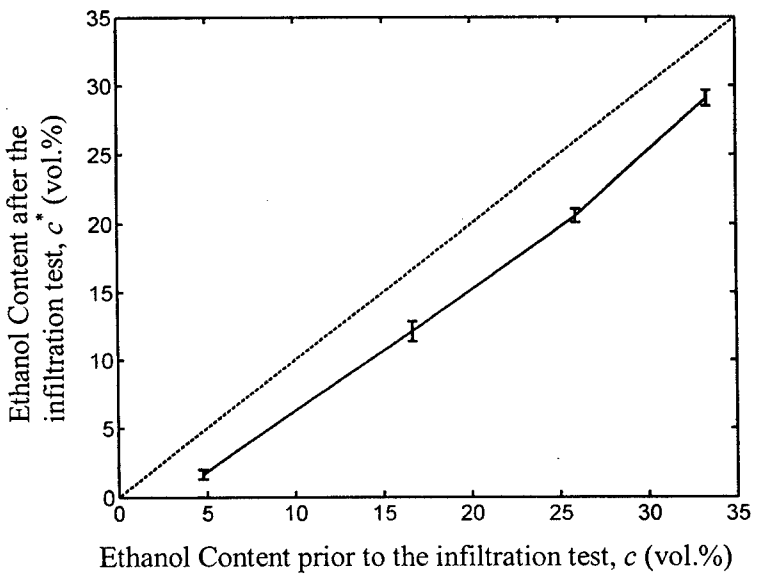

Fig.6 The variation in ethanol content outside the nanoporous particles after the infiltration tests.

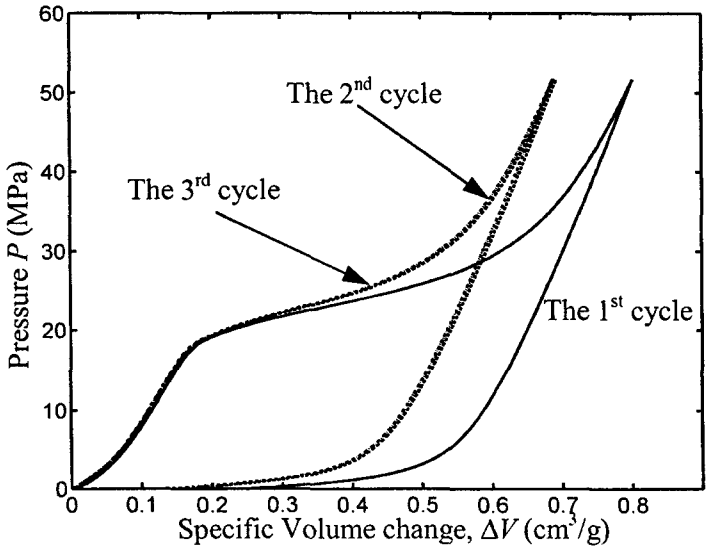

Fig.7 The energy absorption isotherms under a cyclic loading in a 23.1wt% aqueous solution of NaCl.

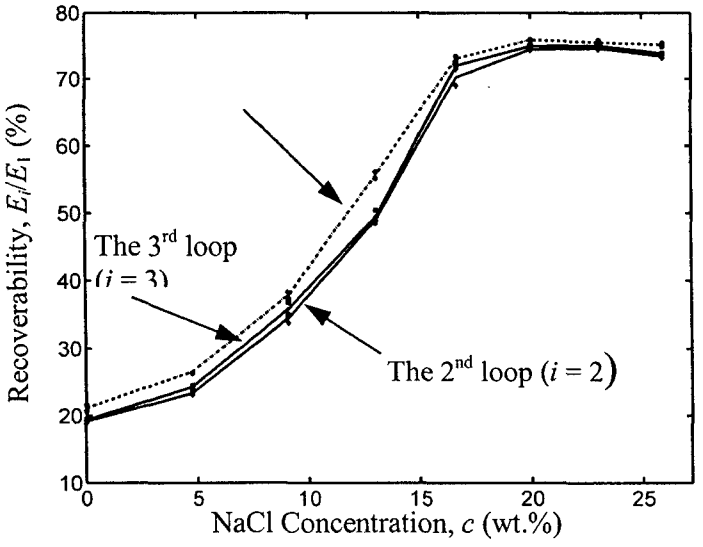

Fig.8 The recoverability as a function of the NaCl concentration of different loading-unloading cycles.

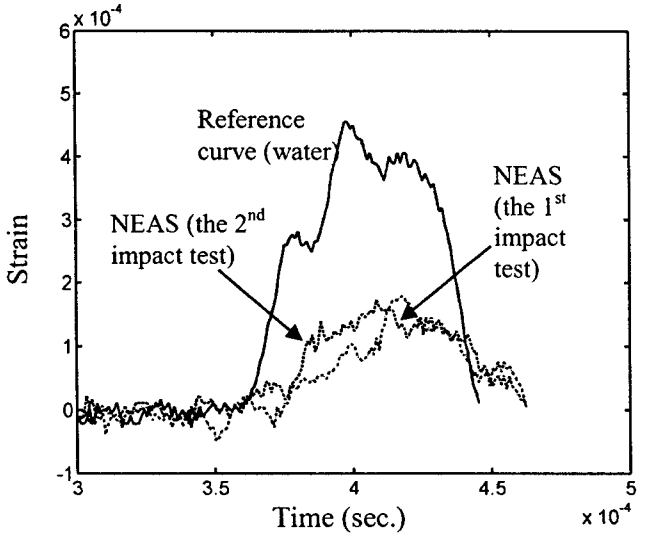

Fig.9 The output pulses of the Hopkinson-bar tests of pure water and NEAS. The curves have been shifted along the horizontal axis.

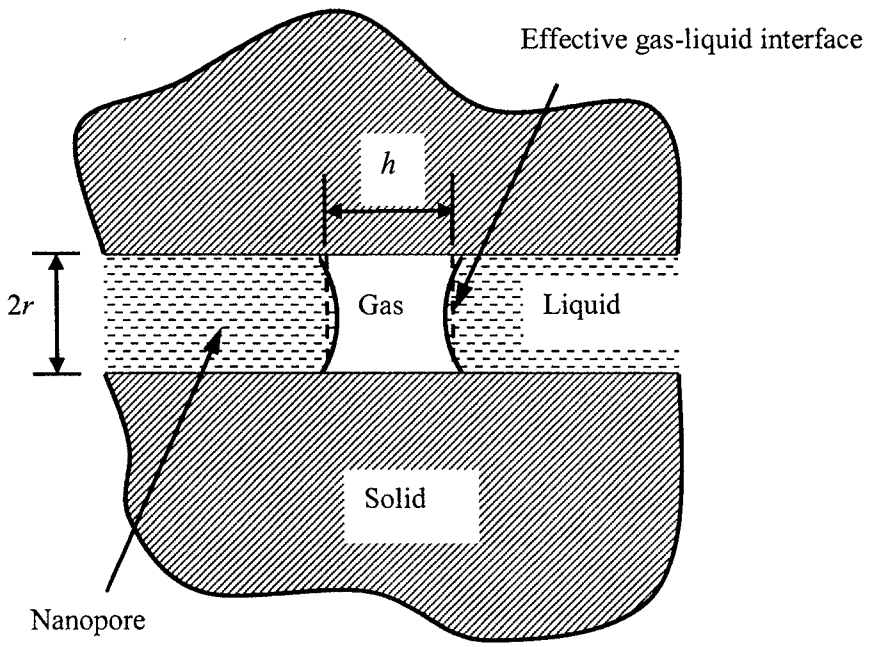

Fig.10 A schematic diagram of the confined phase transformation in a nanopore.

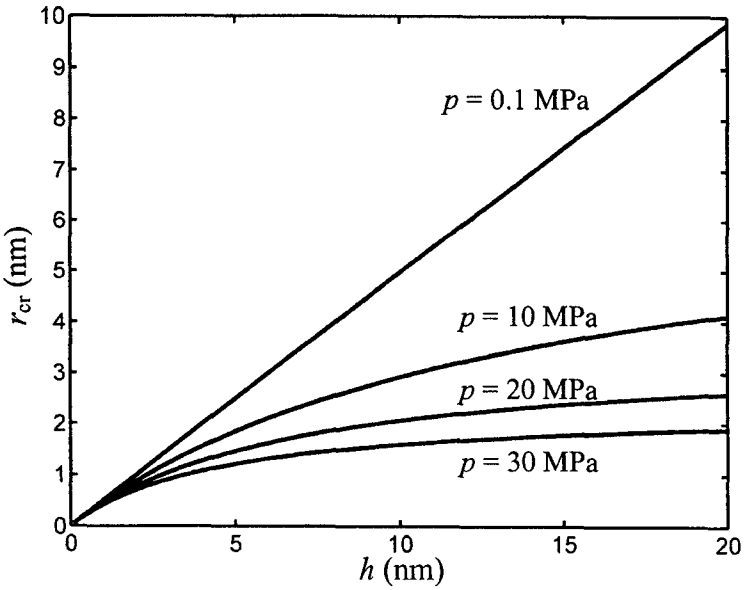

Fig.11 The critical pore size, r_{cr}, as a function of the length of gas phase nucleus, h, and the applied pressure, p.